

# AquaOptical: A Lightweight Device for High-rate Long-range Underwater Point-to-Point Communication (draft)

---

**Marek Doniec, Carrick Detweiler, Iuliu Vasilescu, Mandar Chitre, Matthias Hoffmann-Kuhnt, Daniela Rus<sup>1</sup>**

## Abstract

This paper describes AquaOptical, an underwater optical communication system. Three optical modems have been developed: a long range system, a short range system, and a hybrid system. We describe their hardware and software architectures and highlight trade-offs. We present pool and ocean experiments with each system. In clear water, AquaOptical achieved a data rate of 1.2Mbit/sec at distances up to 30m. In water with visibility estimated at 3m, AquaOptical achieved communication at data rates of 0.6Mbit/sec at distances up to 9m.

## Introduction

Our goal is to develop persistent long-term ocean observatories that can monitor and survey underwater habitats. To this end, we are developing underwater sensor networks (Vasilescu et al., 2005; Vasilescu et al., 2010; Detweiler et al., 2007). An underwater sensor network integrates computation, communication, sensing, and supporting algorithms. Both hardware and software components of the system have to address the characteristics of the sub-sea environment. A critical component of an underwater observatory is its ability to transmit data collected in-situ from sensors. Traditionally, underwater communications used acoustic communications, which achieve long-distance broadcast at slow data rates with high-power consumption. Two examples are the commercially available WHOI acoustic modem (Freitag et al., 2005) and the Benthos modem (Teledyne Benthos, 2010).

In this paper, we investigate optical communication as an alternative to acoustic communication for communication underwater. Optical communication underwater has the potential to achieve much higher data transfer rates than an acoustic communication system at significantly lower power consumption, simpler computational complexity, and smaller packaging. However, they operate in a point-to-point communication setting, where both, the receiver and the transmitter, are usually directional and require alignment for the communication to work effectively. Further, their range and

---

<sup>1</sup> M. Doniec, I. Vasilescu, C. Detweiler, and D. Rus are with CSAIL, MIT. M. Chitre and M. Hoffmann-Kuhnt are with ARL, NUS, Singapore

scope is affected by the water clarity, water light absorption, and power loss due to propagation spherical spreading. We believe that an effective method for uploading large-scale data collected by an underwater sensor network is to use data muling, where a robot equipped with an optical modem will visit each node of the sensor network and upload its data while hovering within optical communication range. In our previous work (Vasilescu et al., 2005), we have built and demonstrated an underwater sensor network system capable of optical data muling. However, the performance of the optical modems was low. This paper describes a second generation optical communication system that improves over the previous version in data rate, range, power use, and capability.

We build on underwater optical communication research by other groups. A number of studies explore the theory of optical transmission in water (Fung et al., 2009; Smart, ; Snow et al., 1992; Cochenour et al., 2006; Laux et al., 2002). An early underwater analog communication system was reported in (Tsuchida et al., 2004). It uses infrared light to transmit crayfish neuronal activity information from live crayfish in an aquarium. There are a few recent studies exploring possible techniques and systems for underwater optical communication (Chancey 2005; Giles et al., 2005; Schill et al., 2004). Farr et al. conclude that using optical communication is the only way to achieve high data rates underwater (Farr et al., 2006). They discuss the possibility of using optical communication for control of underwater vehicles and present the results of an early prototype optical communication system. Using optical communication for controlling underwater robotics swarms is suggested in (Fung et al., 2009). Recently the use of waveguide modulated optical lasers has been proposed for high-speed optical communication (Hanson et al., 2008). They report error-free underwater optical transmission measurements at 1Gbit/s over a 2m path in a laboratory water pipe with up to 36dB extinction. The setup requires an optically pumped 1W laser that is converted to the appropriate wavelength by the use of a PPLN crystal. This makes an omnidirectional transmitter very difficult. Further, the device is large and complex due to the difficulty in directly modulating a green laser at high speed. We reported the first use of optical networking underwater in (Vasilescu et al., 2005; Dunabin et al., 2006). This article builds on a previous version of this work that was presented in (Doniec et al., 2009).

## **AquaOptical Hardware**

We have developed three optical communication systems: the long range optical modem (called AquaOpticalLong), the short range optical modem (called AquaOpticalShort), and a hybrid optical modem (called AquaOpticalHybrid), a cross between the other two. Our goal with this work is to study the space of design and performance for optical modems and identify trade-offs in this space. The long range optical modem has been designed to operate at low power, distances on the order of tens of meters, and communication rates on the order of 1Mbit/sec. The short range optical modem has been designed to operate at distances on the order of 1-5 meters and data rates on the order of 1Mbit/sec. There are significant hardware and software differences between these modems as described in the next sections. The main trade-offs are between cost, distance, and performance.

## Long Range Optical Modem

AquaOpticalLong consists of two components, an optical transmitter and an optical receiver, each of which is contained in water-tight tubes of 8cm diameter and 26.7cm and 38.1cm length respectively. The transmitter weights 1500g and the receiver 2075g. The transmitter consists of an array of six 5W LEDs that emit 480nm light. They can be operated at up to 5MHz with a minimum pulse length of 100ns. An FPGA is used to encode a raw data stream into symbols for the physical layer using DPIM (Discrete Pulse Interval Modulation, see Figure 2). Each byte is converted into four symbols, each of which is represented by a different length pause between two consecutive light pulses. Figure 10 shows an overview of the long range optical modem receiver. The receiver consists of an Avalanche Photo-diode, which includes a low-noise amplifier and is thermo-electrically cooled. An ADC converts the resulting signal into a stream of 12-bit words by sampling at 40 Mega samples per second (MSPS). A primary stage FPGA then filters the digitized data stream. Inside the FPGA the signal is filtered using a Matched Filter (MF) and then digitized into a pulse train using a threshold filter (TF). The digital output from the primary stage FPGA is fed into a secondary stage FPGA, which serializes it into a byte stream. The packets are delimited by a fifth symbol whose pulse length is larger than the other symbols used to encode data. Each packet begins with a 4-byte header consisting of transmitter address, receiver address, packet length and packet type, and terminates with a CRC byte. Figure 1 shows the optical modem prototype. This version of the modem does not include error correction.

A previous version of the AquaOpticalLong receiver utilized a variable gain amplifier (VGA) in conjunction with an analog threshold filter to digitize the incoming signal. We replaced this setup with the ADC and first stage FPGA. In the experimental section of this paper, we refer to this previous version as the AquaOpticalLong with VGA. We refer to the new version as AquaOpticalLong with MF.

## Short Range Optical Modem

The high-level architecture of the short range optical modem is similar to the architecture of the AquaOpticalLong. It includes an optical receiver and an optical transmitter.

The short range receiver uses a commonly available and inexpensive photodiode produced by Advanced Photonix, Inc (part number PDB-C156). The actual sensor of the diode is  $8.02\text{mm}^2$  large and has a response of 14 - 18 A per W of light received. The output of the diode is digitized using an IrDA receiver chip produced by Linear Technology (part number LT1328). Just as with the long range model, the digitized output is decoded using an FPGA and serialized into a byte stream. The packets are delimited by a fifth symbol whose pulse length is larger than the other symbols used to encode data. Each packet begins with a 4-byte header containing transmitter address, receiver address, packet length and packet type, and terminates with a CRC byte.

The short range transmitter consists of one of the units used by the long range optical system, which is a 5W LED that emits 480nm light. An FPGA is used to encode a raw data stream into symbols for the physical layer using DPIM (Discrete Pulse Interval Modulation). Each byte is converted into four symbols, each of which is represented by a different length pulse.

In contrast, the long range receiver uses an array of six LEDs for transmission and an avalanche photodiode which is far more sensitive than the photodiode used in the short range system and much more expensive. The costs of an avalanche photodiode with the primary control circuitry are two orders of magnitude higher than those of a simple photodiode such as the PDB-C156. Thus, the advantages for the PDB-C156 diode and LT1328 combination are:

- small size (see Figure 3),
- easy to use/control,
- low power consumption,
- low heat dissipation,
- and low cost.

Its disadvantages are:

- a worse signal response than the avalanche diode
- and digitization of the signal at an early stage (no low noise amplifier, just a preamp) thus losing possible information.

The advantages for the long range modem are:

- higher sensitivity,
- better amplifiers (this making the detection of very weak pulses possible and increasing communication range.)

The disadvantages are:

- size (more than 10 times the volume of the PDB-C156/LT1328 assembly),
- its power consumption (5W for cooling and additional power for control),
- the resultant heat dissipation which requires active cooling and a large heat sink,
- and, finally, its significantly higher cost.

## Hybrid Optical Modem

We designed the hybrid optical modem to enhance the performance of the short range modem by using the more powerful transmitter of the long range system and the lower cost receiver of the short range system.

## AquaOptical Software

The software of AquaOptical consists of two modules: the symbol encoder/decoder and the packet encoder/decoder. The symbol encoder is located inside the FPGA, the packet encoder and decoder run on the CPU of the sensor node, while the symbol decoder is split between the FPGA and the CPU of the sensor node.

The packet encoder takes payload data of 1 - 250 bytes and a destination byte as input. It constructs a valid packet by creating the 4-byte header (source, destination, type, and length) as well as computing and appending the CRC byte. It then sends the packet over a serial peripheral interface (SPI) bus to the symbol encoder located inside the FPGA.

The symbol encoder receives each packet as a stream of bytes as input. Each byte is split into 4 bit-pairs. The packet is processed first to the last byte. The MSB of each byte are processed first, the LSB last. The first light pulse sent marks the beginning of the packet. A synchronous counter running at 16MHz times the distances between successive light pulses to encode the symbols. The duration of the light pulses generated as well as of the different pauses used for the 4 possible symbols can be configured in software.

The symbol decoder front end is running inside the FPGA. It takes as input the digitized output of the photodiode. When the first pulse is received, a new decoding cycle starts. A 16MHz counter times the distance between successive pulses. After each pulse, the new distance is stored inside a FIFO. If the distance counter exceeds the maximum count (255), the value 255 is written into the FIFO and the counter simply waits for the next pulse to start.

The actual decoding of the symbols takes place inside the CPU. The CPU polls the bytes from the FPGA using the SPI bus. Each distance is converted into a bit-pair using software configurable threshold values. Every 4 successive bit-pairs are packed into a byte, which is written into a buffer. When a distance larger than a packet timeout threshold is read, the packet decoder is called to process the current buffer contents.

The packet decoder checks if the CRC of the buffer is 0 and if the packet is addressed to this sensor node. It then calls the handler for the data.

The FPGA contains the symbol layer encoder and front end of the decoder in order that both can run asynchronously to the CPU. Additionally, this ensures that packet encoding and decoding are not influenced by other processes running on the same CPU.

## **Power Consumption**

All three versions of AquaOptical share the same sensor node design and thus the same energy source design. Each device contains 6 Lithium Polymer (LiPo) Cells with a capacity of 9.62Wh (3.7V, 2.6Ah). The cells are arranged in a 3x2 configuration yielding an average voltage of 11.1V and a capacity of 5.2Ah or 57.72Wh. This energy has to be shared between the sensor board and the communication hardware of the optical modem (LEDs, drivers, APD, amplifiers, decoder).

The sensor board consumes an average of 100mW when running in active mode without radio and GPS enabled. It can sleep when not receiving data, at which point it consumes about 1mW.

## **Power Consumption for the Transmitter**

The AquaOpticalShort transmitter design drives a single LED at 5W strong pulses. The current limiting resistor drops an additional 1.4W, resulting in a total pulse power of 6.4W. The current encoding

architecture pulses the LEDs at an average duty cycle of 1/3, resulting in an average power consumption of 2.1W. Together with the sensor board, this results in a total power consumption of 2.2W and a theoretical run time of over 26 hours.

The AquaOpticalLong transmitter utilizes six of the same LEDs resulting in a total power consumption of 12.9W and a theoretical run time of 4:28 hours.

There are multiple ways to extend this run time. Some of these only require software changes, some extensions to the hardware.

The easiest method is to drop the duty cycle significantly. We currently run the modem with a 1/3 duty cycle at 600Kbps resulting in an average pulse length of 1 $\mu$ s. This length was chosen to enable easier measurement of pulses and distinguish them from ambient noise. Changing pulse width can be done in software and requires a change in the FPGA programs for both encoder and decoder. The theoretical limit is the minimum time it takes for the LEDs to switch fully on, which we measured to be around 100ns. Since every pulse carries two bits of information, we can express a simple relationship between data rate and power consumption. For AquaOpticalLong, this relationship for the current encoding scheme (DPIM) is 3.84W/Mbps given a pulse length of 100ns. The maximal theoretical data rate resulting from 100ns pulse width and DPIM is 3.3Mbps, resulting in a power consumption of 12.8W. However, if we run the modem at 600Kbps with 100ns pulses, our power consumption drops to 2.4W total, resulting in a theoretical run time of 24 hours.

## Power Consumption for the Receiver

The AquaOpticalShort receiver consumes below 20mW, which is less than the sensor node itself. This design can theoretically operate for over 20 days.

The AquaOpticalLong receiver consumes power for three different tasks. The first is the cooling of the APD, which, according to specifications consumes, between 4W and 9.5W depending on the cooling needed. The second is the drive circuitry for the APD together with the LNA, which, according to specifications, consumes between 1.8W and 3.2W. Finally, the decode stage (matched filter, pulse detection) consumes 100mW to drive the analog to digital converter (ADC) and the FPGA, which runs the matched filter and pulse detector. We measured the power consumption of the entire receiver system to be 6W in complete darkness, 7.2W at ambient office light levels, and 15W when saturated by a halogen light.

When the receiver is actually operating, its power consumption lies in the range between the ambient light measurement and the saturated sensor measurement. Thus, we predict runtime to be 4h in the worst case scenario.

As with the transmitter, there are multiple ways to improve runtime for the receiver. First, a better optical filter can be used that lets a narrower bandwidth of light pass. This has to be well tuned with the transmitting LEDs. The current filter was chosen to well cover the entire emission spectrum of the chosen LEDs and is 20nm wide. However, if the light source were to be confined to a smaller band gap like 10nm, then a 10nm filter would halve the amount of ambient light polluting the sensor. This would directly result in a significant cooling costs reduction. Assuming that the APD heats up linearly with incident light, then cooling power consumption could be cut by up to half.

Another way to reduce energy is to use a form of time domain multiple accesses in which the APD is switched on for certain time windows during which a request for data transfer has to be sent. This could reduce heat-buildup in the APD and would again cut cooling power consumption. As an example, the request windows could be 10ms long in each 100ms interval, resulting in a 10% duty cycle when no transfers are requested. The disadvantage of this method is, however, the increased latency and the need for synchronized clocks between transmitter and receiver.

## Experiments

We implemented and packaged the AquaOptical systems. We conducted several experiments in air, in the pool and in the ocean in Singapore Harbor.

### Air Transmission Experiment

The air transmission experiments were done in an urban environment on the MIT campus. This experiment was conducted after dark to avoid sensor saturation through direct sunlight exposure. Significant ambient noise was present from street lamps and light from buildings. We only tested the AquaOpticalLong utilizing a matched filter (MF). Two scientists held and aimed the transmitter and receiver at each other. The optical modem recorded data transmission with 100% success rates at a data rate of 1.2Mbit/sec and distances up to 160m. The transmission success rate decreased to 70% at 200m, which was the maximum measured distance.

### Pool Experiments

The pool experiments were performed in clear water. The optical modem recorded data transmission with 100% success rates at data rates up to 1.2Mbit/sec for all the distances tested. In this set of experiments, the maximum distance tested was 30m due to the dimensions of the pool in which we conducted the experiments. We expect good optical communication performance in clear waters at distances up to 50m.

## Field Experiments in the Ocean 1

Four sets of field experiments were conducted in the ocean at a location between outlying islands south of Singapore. The big challenge for these experiments was achieving optical communication in low visibility environments. At the experimental site, human divers estimated the water visibility to be 3m for the first three sets and 1.5m for the last experiment. The goals of these experiments were:

1. To measure the success rate of the long range optical modem system with a variable gain amplifier at various distances up to 10m.
2. To measure the success rate of the short range optical modem system at various distances up to 3m using blue and green light for comparison.
3. To measure the success rate of the hybrid optical modem system consisting of the long range sender and the short range receiver. Since the short range modem system is much less expensive than the long range system, such a hybrid configuration might be used for data muling with a robot carrying the long-range receiver and a sensor network with multiple nodes equipped with the short range receiver.
4. To measure the success rate of the long range optical modem system with a matched filter receiver at various distances up to 10m.

## Experimental Setup

We conducted a suite of experiments to evaluate the performance of the three optical modem systems described in this paper in the ocean. The first three experiments were conducted near a barge south of the Singapore Harbor. The water visibility during these experiments was estimated by human divers at 3m. Figure 4 shows the basic experimental setup for the field evaluations of the optical modems. For the short range experiments, we suspended a rigid 4m long rod below the boat at a depth of 4m measured from the top of the water. Prior to submersing the rod, we measured and marked distances on the rod in 50cm increments. Two divers were used in each experiment. One diver carried the transmitter unit and the other carried the receiver unit. The divers were connected to the researchers on the boat using an audio communication system integrated in the diving mask. The receiver was connected to a computer on the boat in order to provide visual feedback about the experiment and debugging information. The diver holding the receiver was instructed to hold the receiver parallel to the rod at position 0. This diver maintained this location for the duration of the experiment. The diver holding the transmitter was given a series of voice instructions. He was first instructed to go to the position marked 1m (which was measured to be 1m away from the fixed receiver) and hold the transmitter parallel to the rod, aimed at the receiver. He maintained this position for one minute and data was collected for 30 seconds at a data rate of 0.6Mbit/sec. The diver was then instructed to move further back in 50cm increments, each time maintaining the transmitter position at the current location for approximately one minute.

A similar experiment was conducted for the long range optical modem. Since our expectation in this case was communication at a much further distance than in the short range evaluations, we used a rope instead of a rod. The use of a rope allowed us to point the receiver and transmitters at each other at distances greater than what the human eye could see. We attached the rope used to measure the



distance between the long range optical modem transmitter and receiver to a vertical rope that was fixed to the boat and kept taut by weights. The first diver with the receiver was stationed at the attachment point of the measuring rope to the vertical rope. He pointed the receiver along the measuring rope. The second diver who was holding the transmitter moved along the measuring rope and pointed the transmitter along the rope in the direction of the receiver. The measuring rope was kept taut by the water currents present.

The fourth and final experiment was conducted off the dock at the Republic of Singapore Yacht Club. The water visibility was estimated to be 1.5m by lowering the optical modem on a rope until it was no longer visible. The experimental setup can be seen in Figure 4. The transmitter and receiver were mounted to metal L-shaped brackets that were connected with a rope to set a distance between the modems. Each bracket was further held by a depth-rope that allowed us to adjust both depth and the tension on the distance-rope. A 10KG weight was attached with a rope to each bracket. By moving the fixture points of the depth-ropes on the dock, we were able to adjust the angle at which the transmitter and receiver were aimed. Depth could also be adjusted with the depth-ropes. The disadvantage of this setup was that once the modems were out of sight (because of water turbidity) we could only estimate the angle at which they were aimed.

### **Short Range Optical Modem Evaluation Data**

Specifically, for the short range experiments, a single 5 Watt LED was used in the transmitter. Two experiments were conducted: one with a blue LED (470nm) in the transmitter and one with a green LED (530nm). The radiant flux generated by the LEDs is roughly equivalent to 10% of the power input, or 500mW. The receiver uses an off-the-shelf photodiode. The short range experiments were conducted with a throughput of 1.2Mbit/sec or 1.75uS/symbol average.

All experiments were conducted at 4m water depth. For the short range experiments, a 4m long pole was suspended off the boat to float horizontally at 4m depth in alignment with the water current. The short range receiver was mounted at one end of the pole and pointed along the pole. It was tethered through a cable to allow for supervision and data logging. A measuring tape was attached to the pole. A diver was holding the transmitter and positioning it at the appropriate distances along the pole. The diver tried at all times to point the modem along the pole. At each recorded distance, the diver stayed for at least 20 seconds and continuously pointed the transmitter along the pole towards the receiver. Measurements were taken and binned in 2 second intervals. Each measurement consisted of the number of valid packets received and a histogram of pulse lengths received in that 2 second interval.

Figure 5 shows the experimental data with the short range optical modem using green (green lines) and blue (blue lines with circles) light. We expected to see blue light outperform the green light as predicted by the literature. However, we observed green light to be more effective in Singapore waters. We believe this is due to the water color in the Singapore Harbor and surrounding areas.

The dashed lines correspond to the percentage of valid pulses received (corresponding to a symbol) divided by the total number of pulses received. Bad pulses are due to ambient noise. The solid lines

show the number of valid packets received divided by the total number of packets received. Packets were 128 bytes long. Valid packets are those addressed correctly with matching CRCs.

### **Long Range Optical Modem Evaluation Data**

For the long range experiments, six 5W blue (470nm) LEDs were used in the transmitter and an avalanche photodiode with a VGA was used in the receiver. The radiant flux on the transmitter was 3W. The first set of long range experiments was conducted with a throughput of 666Kbits or 3uS/symbol average. The second set of long range experiments was conducted with a throughput of 333Kbits or 6uS/symbol average.

The long range experiments were conducted in a similar fashion as the short range experiments. However, we replaced the 4m pole with a 12m rope with 1m markings that was tied to the receiver. The other end of the rope was not tethered and was floating in the current (up to 2m/s). A diver held the receiver and tried to point it along the rope at all time. A second diver held the transmitter and was holding on to the rope while trying to point the transmitter along the rope. The rope was straight at all times due to the strong current pulling the second diver and thus straightening the rope. It was the second diver's responsibility to keep a depth of 4m. Measurements were conducted in the same fashion as with the short range receiver. Figure 6 shows the experimental data with the long range optical modem taken on two different days (using blue light).

Similar to Figure 5, in Figure 6 the dashed lines correspond to the percentage of valid pulses received divided by the total number of pulses received and the solid lines show the number of valid packets received divided by the total number of packets received. For the long range receiver, bad pulses are due to both ambient noise and noise inside the receiving circuit due to the VGA.

An additional set of ocean experiments was conducted for the AquaOpticalLong with a matched filter decoder. The AquaOpticalLong with MF was tested in harbor water with a visibility of about 1.5m where it achieved a transmission distance of up to 8m (5 times visibility) at a data rate of 600Kbps. In comparison, the transmission maximum distance for the experiments conducted with the variable gain amplifier version of the long range modem was 9m but water visibility was only 3m. Therefore, the MF version of the long range modem achieved 5 times visibility and the VGA version 3 times visibility. The results can be seen in Figure 7. The experiments demonstrated that the matched filter design not only improved signal detection, but also almost entirely removed false positive detection of signal pulses. This can also be seen in Figure 7 where the success rate remains 0 after the maximum transmission distance. The previous design showed reception artifacts because of a high false positive rate of the variable gain amplifier design.

### **Hybrid Modem Evaluation Data**

During the long to short range experiments, we used a short range receiver (off the shelf photodiode) with our long range 3W radiant flux transmitter. The same procedure as in the long range experiment was used in this case.

Figure 8 shows experiments carried out during the second day using the long range optical modem transmitter and the short range optical modem receiver. The blue dashed line corresponds to the percentage of valid pulses received divided by the total number of pulses received. Bad pulses are again due to both ambient noise and noise inside the receiving circuit due to the VGA. The red line is the number of valid packets received divided by the total number of packets received, were packets were again 128 bytes long and valid packets are those addressed correctly and with matching CRCs.

## Discussion

Figure 9 shows the time history of one experiment. We can see how the diver conducting the experiment moved first away and then closer to the sender during the experiment. You can also see a very clear peak where the packets start arriving. The portion of the graph before the peak is noise occurring while the diver moved into position. This noise is the result of the variable gain amplifier adjusting to noise levels when no valid signal is present. This problem no longer occurs in the matched filter design of the long range optical receiver.

For each distance interval, the packet and symbol success rate were measured for 30 seconds. The testing rate for the data transfer was 600Kbit. Under these harsh visibility conditions, the long range optical modem achieved very close to perfect transmission rates up to 8m. The performance degrades, but is still operational up to 9.5m. At 10m, the receiver does not pick up any symbols.

These experiments demonstrate that the optical communication system is very well suited for data transfer at large distances (e.g. 25m) in clear waters. The data transfer rate was good at twice the visibility range in turbid waters. We believe AquaOptical is an encouraging first step toward creating an effective optical communication system for use in data muling and other underwater data transfer scenarios. Next steps include hardware redesign for power optimization and the development of a software layer capable of both error correction and higher-level interfacing to the system.

## Conclusion

This paper discussed the design of a family of three underwater optical modem systems. We have designed and built three systems: a long range optical modem, a short range optical modem, and a hybrid optical modem. We analyzed the trade-offs between these systems and characterized their performance in the pool and in the ocean. Our preliminary experimental results suggest several hardware and software improvements to the system as well as additional experimental characterization. Our current efforts are focused on the software side to include error correction in the symbol processing and on the experimental side to evaluate the sensitivity of the systems to orientation. Next we plan to use the optical modem systems for data transfer between sensor networks equipped with the short range modem transmitter and receiver, and a robot equipped with the long range modem transmitter and receiver.

## Acknowledgments

This work was supported by DSTA, Singapore and the MURI Antidote project. We are grateful for this support. We are also grateful to the team at ARL, National University of Singapore, for providing logistical and technical support for our experiments.

## Bibliography

Channey M., A. 2005. Short range underwater optical communication links. Master's thesis, North Carolina State University. 117 pp.

Cochenour B., Mullen L., Laux A., and Curran T. 2006. Effects of multiple scattering on the implementation of an underwater communications link, In: Proc. of MTS/IEEE OCEANS, pp. 1–6. Boston, MA, USA.

Detweiler C., Vasilescu I., and Rus D. 2007. An underwater sensor network with dual communications, sensing, and mobility. In: Proc. of OCEANS - Europe, pp 1-6. Aberdeen, Scotland.

Doniec M., W., Vasilescu I., Detweiler C., Rus D., Chitre M., Hoffmann-Kuhnt M. 2009. AquaOptical: A Lightweight Device for High-Rate Long-Range Underwater Point-to-Point Communication. In: Proc. of MTS/IEEE OCEANS. Biloxi, MS, USA.

Dunbabin M, Corke P., Vasilescu I., and Rus D. 2006. Data muling over underwater wireless sensor networks using an autonomous underwater vehicle. In: Proc. of IEEE International Conference on Robotics and Automation, ICRA, pp 2091–2098. Orlando, FL, USA.

Farr N., Chave A., Freitag L., Preisig J., White S., Yoerger D., and Sonnichsen F. 2006. Optical modem technology for seafloor observatories. In: Proc. of MTS/IEEE OCEANS, pp 1-6. Boston, MA, USA.

Freitag L., Grund M., Singh S., Partan J., Koski P., and Ball K. 2005. The WHOI micro-modem: an acoustic communications and navigation system for multiple platforms. In: Proc. of MTS/IEEE OCEANS, pp 1086-1092. Washington DC, USA.

Fung Y., F. and Ercan M., F. 2009. Underwater short range free space optical communication for a robotic swarm. In: Proc. of International Conference on Autonomous Robots and Agents, ICARA, pp 529-532. Wellington, New Zealand.

Giles J., W. and Bankman I., N. 2005. Underwater optical communications systems. part 2: basic design considerations. In: Proc. of IEEE Military Communications Conference, MILCOM. pp 3:1700-1705. Atlantic City, NJ, USA.

Hanson F. and Radic S. 2008. High bandwidth underwater optical communication. J. Appl. Opt., 47(2):277–283.

Laux A., Billmers R., Mullen L., Concannon B., Davis J., Prentice J., and Contarino V. 2002. The a, b, cs of oceanographic lidar predictions: a significant step toward closing the loop between theory and experiment. *J. of Modern Opt.*, 49(3/4):439-451.

Schill F., Zimmer U., R., and Trumpf J. 2004. Visible spectrum optical communication and distance sensing for underwater applications. In: *Proc. of Australasian Conference on Robotics and Automation, ACRA*. Canberra, Australia.

Smart J., H. 2005. Underwater Optical Communication Systems. Part 1: Variability of Water Optical Parameters. In: *Proc. of IEEE Military Communications Conference, MILCOM*. pp 2:1140-1146. Atlantic City, NJ, USA.

Snow J., P., Flatley J., P., Freeman D., E., Landry M., A., Lindstrom C., E., Longacre J., R., and Schwartz J., A. 1992. *J. Appl. Opt.*, 47(2):277-283.

Teledyne Benthos. 2010. Undersea, Geophysical Equipment, Survey Sonar and ROV. <http://www.benthos.com>.

Tsuchida Y., Hama N., and Takahata M. 2004. An optical telemetry system for underwater recording of electromyogram and neuronal activity from non-tethered crayfish. *J. Neuroscience Methods*, 137:103-109.

Vasilescu I., Detweiler C., Doniec M., W., Gurdan D., Sosnowski S., Stumpf J., Rus D. 2010. AMOUR V: A Hovering Energy Efficient Underwater Robot Capable of Dynamic Payloads, *Int. J. of Robotics Research*, 29(5):547-570.

Vasilescu I., Kotay K., Rus D., Dunbabin M., and Corke P. 2005. Data collection, storage, and retrieval with an underwater sensor network. In: *Proc. of the 3rd international conference on Embedded networked sensor systems, ACM SenSys*, pp. 154–165, New York, NY, USA.



Figure 1: The receiver and transmitter of AquaOpticalLong

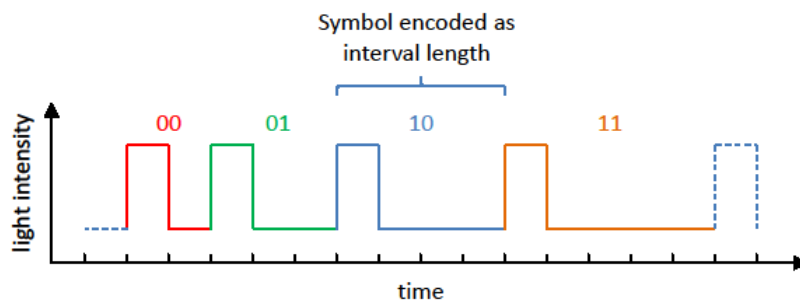


Figure 2: DPIM (discrete pulse interval modulation): Each bit pair is represented by a different distance between two successive light pulses.



Figure 3: The receiver and transmitter of AquaOpticalShort can be seen on the left. A sensor node with the short range receiver and transmitter integrated in the top cap is displayed on the right.

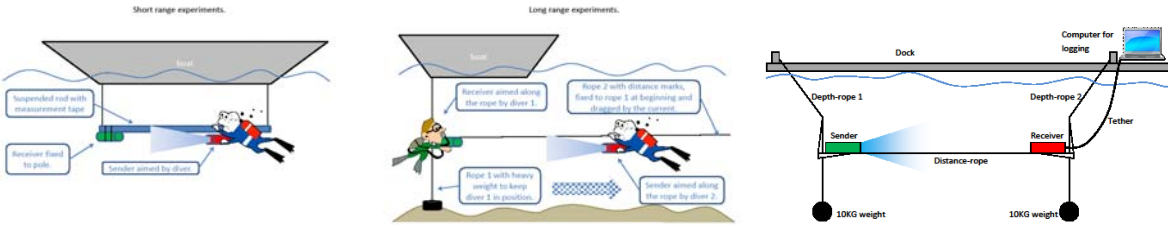


Figure 4: LEFT: Experimental Setup for the Long Range VGA optical Modem evaluation. MIDDLE: Experimental Setup for the Short Range optical Modem evaluation. RIGHT: Experimental setup for the Long Range MF optical Modem evaluation.

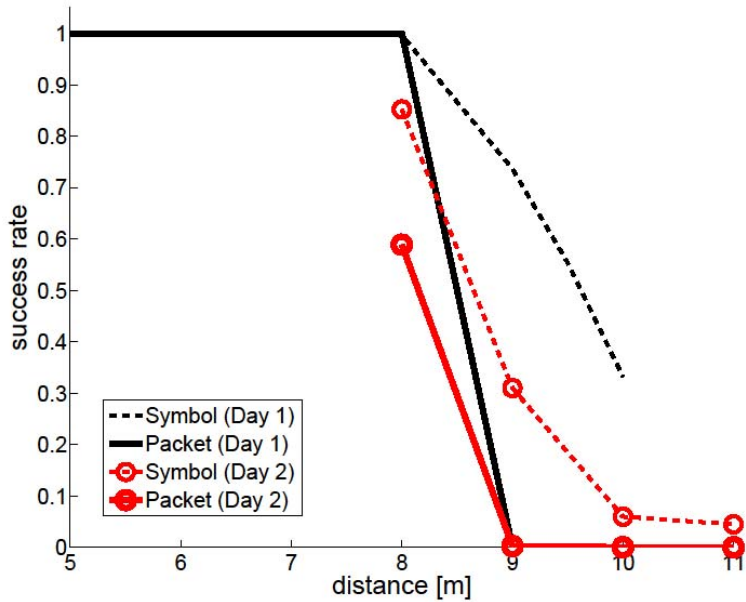


Figure 6: Singapore Optical Modem Experiment: Long Range (VGA) symbol and packet success rate using blue light. The x axis corresponds to distance. The y axis shows the percentage of valid pulses received (dotted lines) and valid packets received (solid lines). The black lines show results of the first day and the red lines (with circles) to the results of the second day.

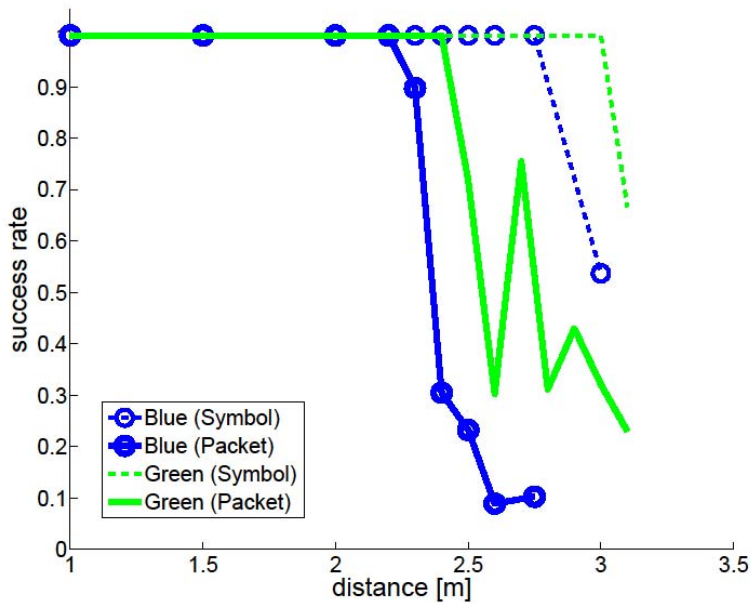


Figure 5: Singapore Optical Modem Experiment: Short Range symbol and packet success rate using blue and green light. The x axis corresponds to distance. The y axis shows the percentage of valid pulses received (dotted line) and valid packets received (solid line). The blue lines (with circles) show results from trials using blue light. The green lines show results from trials with green light. Artifacts caused by the decoding of noise that when no signal is present have been removed in this plot for clarity.



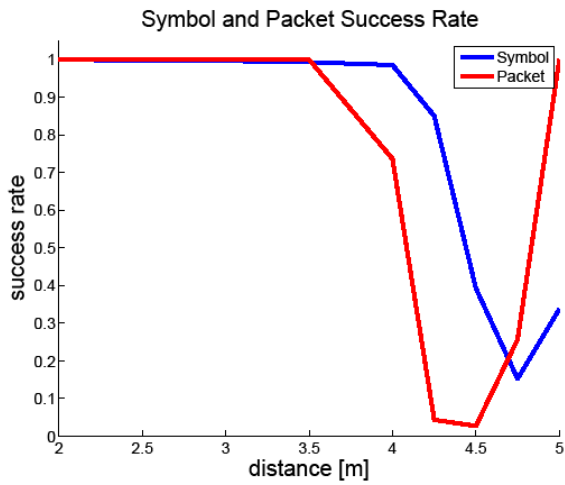


Figure 8: Singapore Optical Modem Experiment: Hybrid Modem success rates using the long range optical modem sender and the short range optical modem receiver using blue light. The x axis corresponds to distance. The y axis shows the percentage of valid pulses received (blue dashed line) and valid packets received (red line).

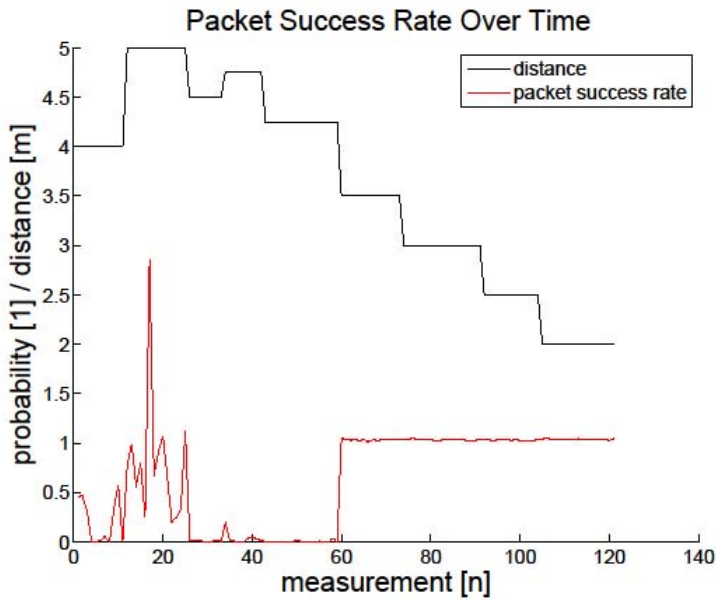


Figure 9: The timeline of a Hybrid Optical Modem experiment. The x axis corresponds to discrete 2 second-long measurements. From left to right, we see the history of the experiment. The y axis is the packet success rate (in red) and distance (in black).

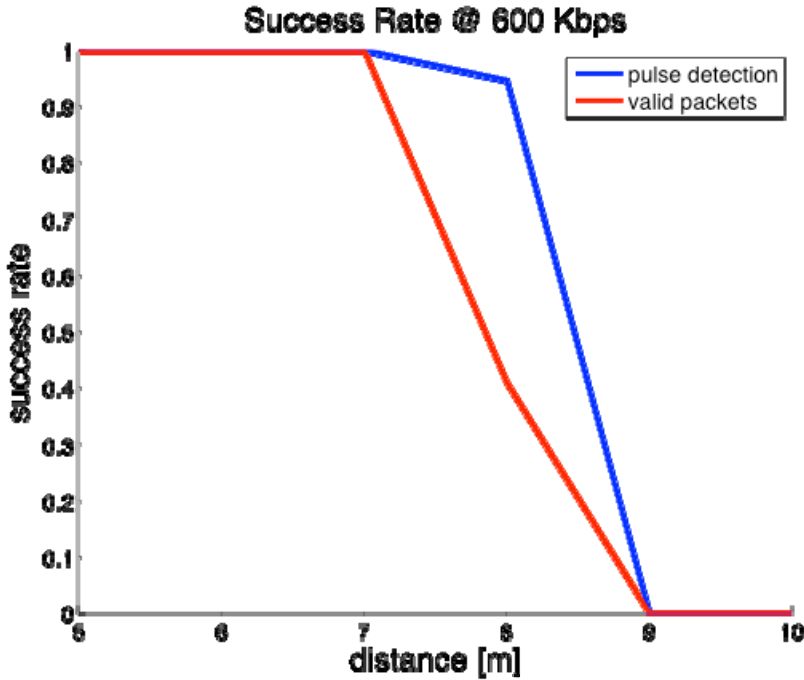


Figure 7: Singapore Optical Modem Experiment: Long Range (MF) symbol and packet success rate using blue light. The x axis corresponds to distance. The y axis shows the percentage of valid pulses received (blue dashed line) and valid packets received (red line).

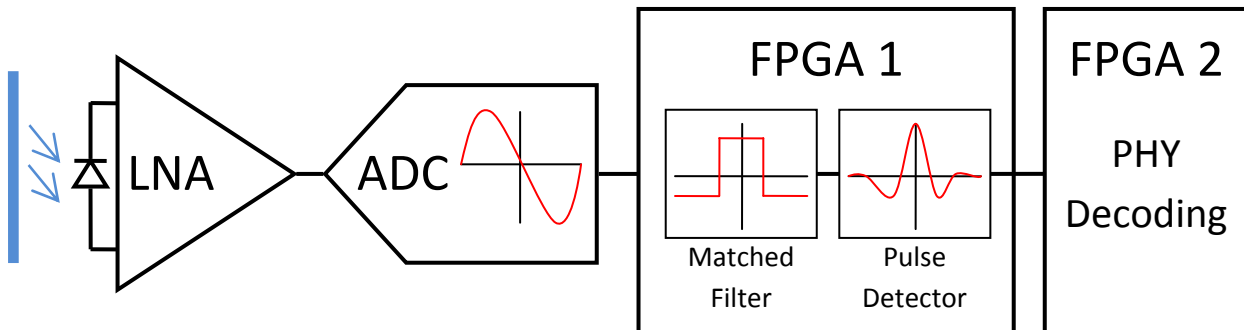


Figure 10: The Long Range Optical Modem Receiver using a Matched Filter (MF). The incoming signal is first digitized at up to 40 Mega samples per second. A matched filter corresponding to the expected pulse shape is then applied to the signal. Finally a Threshold Filter is used for pulse detection.